Quantifying the low bias of CALIPSO's column aerosol optical depth due to undetected aerosol layers

Man-Hae Kim[1,2], Ali H. Omar[1], Mark A. Vaughan[1], David M. Winker[1], Charles R. Trepte[1], Yongxiang Hu[1], Zhaoyan Liu[1,3], Sang-Woo Kim[4]

[1] *NASA Langley Research Center, Hampton, VA, USA*

[2] *Universities Space Research Association, Columbia, Maryland, USA*

[2] *Science Systems and Applications, Inc., Hampton, VA, USA*

[4] *School of Earth and Environmental Sciences, Seoul National University, Seoul, Korea*

Correspondence to: Man-Hae Kim (man-hae.kim@nasa.gov)

Key Points:

Global mean (median) lidar ratio for undetected layers is found as 32.62 (28.75) sr from the MODIS AOD constrained retrieval

Global mean ULA retrieved using the lidar ratio of 28.75 sr is 0.031 ± 0.052

ULA is very sensitive to the lidar ratio which a significant source of error

Abstract

The CALIOP data processing scheme only retrieves extinction profiles in those portions of the return signal where cloud or aerosol layers have been identified by the CALIOP layer detection scheme. In this study we use two years of CALIOP and MODIS data to quantify the aerosol optical depth of undetected weakly backscattering layers. Aerosol extinction and column-averaged lidar ratio is retrieved from CALIOP Level 1B (Version 4) profile using MODIS AOD as a constraint over oceans from March 2013 to February 2015. To quantify the undetected layer AOD (ULA), an unconstrained retrieval is applied globally using a lidar ratio of 28.75 sr estimated from constrained retrievals during the daytime over the ocean. We find a global mean ULA of 0.031 ± 0.052. There is no significant difference in ULA between land and ocean. However, the fraction of undetected aerosol layers rises considerably during daytime, when the large amount of solar background noise lowers the signal to noise ratio (SNR). For this reason, there is a difference in ULA between day (0.036 ± 0.066) and night (0.025 ± 0.021). ULA is larger in the northern hemisphere and relatively larger at high latitudes. Large ULA for the Polar Regions is strongly related to the cases where the CALIOP Level 2 Product reports zero AOD. This study provides an estimate of the complement of AOD that is not detected by lidar, and bounds the CALIOP AOD uncertainty to provide corrections for science studies that employ the CALIOP Level 2 AOD.

Index Terms: 0305

Keywords: CALIPSO, aerosol optical depth, lidar ratio, undetected layer, aerosol extinction

1. Introduction

The Cloud-Aerosol Lidar with Orthogonal Polarization (CALIOP) is a space-borne lidar flying onboard the Cloud-Aerosol Lidar and Infrared Pathfinder Satellite Observations (CALIPSO) mission. CALIPSO was launched in 2006 and has produced vertical profiles of aerosols and cloud optical properties over the globe for more than ten years [*Winker et al.*, 2010]. CALIOP aerosol products are widely used for aerosol studies such as aerosol long range transport [e.g., *Huang et al.*, 2008; *Liu et al.*, 2008; *Uno et al.*, 2009, *Yumimoto et al.*, 2009], validation of and assimilation in aerosol models [e.g., *Koffi et al.*, 2012; *Kim et al.*, 2014; *Pan et al.*, 2015; *Sheng et al.*, 2015; *Sekiyama et al.*, 2010], estimation of aerosol radiative effect [e.g., *Huang et al.*, 2009; *Oikawa et al.*, 2013; *Anderson et al.*, 2015; *Matus et al.*, 2015], and aerosol above cloud (AAC) effects [e.g., *Chand et al.*, 2009; *Kacenelenbogen et al.*, 2014; *Liu et al.*, 2015].

Since CALIPSO launched, many studies have been conducted to validate both CALIOP Level 1B and 2 Products. Validation studies show that the version 1 CALIOP Level 1B Product agrees reasonably well with ground-based or airborne lidar measurements [e.g., *McGill et al.*, 2007; *Kim et al.*, 2008]. *Mamouri et al.* [2009], *Mona et al.* [2009], and *Pappalardo et al.* [2010] compared the total attenuated backscatter at 532 nm from CALIOP with ground-based lidar measurements from EARLINET (European Aerosol Research Lidar Network; *Bösenberg et al.*, 2003) and found that CALIOP Version 2.0 data was biased low in the free troposphere (above 3 km) and lower in the planetary boundary layer (PBL). Comparisons with airborne High Spectral Resolution Lidar (HSRL) showed that CALIOP version 3 total attenuated backscatter (TAB) at 532 nm agrees well with collocated HSRL measurements not only for the free atmosphere but for the PBL as well [*Rogers et al.*, 2011]. Initial assessments of the CALIOP version 4 level 1B data show excellent agreement with the HSRL data set [*Toth et al.*, 2106].

Level 2 Products show poor agreement in aerosol optical depth (AOD) with ground-based, airborne, and space-borne measurements. Although there are differences in magnitude, most studies report that CALIOP AOD is biased low [e.g., *Kacenelenbogen et al.*, 2011; *Kittaka et al.*, 2011; *Redemann et al.*, 2012; *Schuster et al.*, 2012; *Kim et al.*, 2013; *Omar et al.*, 2013]. Several studies have attributed the low bias to the lidar ratios used in the CALIOP aerosol retrieval. *Wandinger et al.* [2010] found CALIPSO dust extinction coefficient values are about 30% lower than those obtained from collocated ground-based Raman lidar retrievals, and attribute this finding to multiple scattering effects which are not accounted for in CALIOP inversions. *Schuster et al.* [2012] showed that the CALIOP AOD for dust has low bias (-29%) compared to AERONET (Aerosol Robotic Network) and that lidar ratios than higher than the 40 sr used in CALIOP retrievals for dust are typically retrieved from AERONET measurements (e.g., 49.7 sr in the Sahel, 42.6 sr in the Middle East, and 49.7 sr at Kanpur, India). *Oo and Holz* [2011] found that the CALIOP lidar ratio in marine environments is often low and the CALIOP-derived AOD bias is correlated with the aerosol particle size retrieved by the Moderate Resolution Imaging Spectroradiometer (MODIS).

On the other hand, *Rogers et al.* [2014] reported that lidar ratios retrieved from the airborne HSRL measurements during the CALIOP validation flights in the North America are lower than the CALIOP values except for marine and clean continental aerosols. Moreover, they found that, while the CALIOP column AODs are generally biased low, the CALIOP layer AODs are almost always higher than HSRL AODs. This implies that undetected weakly backscattering aerosols in the free atmosphere offer a more plausible reason for the low bias of the CALIOP column AOD than the underestimation of lidar ratio. *Rogers et al.* [2014] found that CALIOP underestimates column AOD by ~0.02 due to the undetected aerosols in the free atmosphere over the North American and

Caribbean regions at night. *Kacenelenbogen et al.* [2014] also report a similar result but for aerosol-above-cloud (AAC). They note that CALIOP detects AAC only in ~23% of the cases in which it is observed by airborne HSRL. In some cases CALIOP fails to detect aerosol in the PBL. *Kim et al.* [2013] found that the marine boundary aerosols below the elevated smoke layers are frequently undetected by the CALIOP layer detection algorithm due to attenuation, which leads to underestimation of CALIOP AOD for smoke aerosols. *Thorsen and Fu* [2015] also showed that CALIOP detects significantly less aerosol layers for the mid and lower atmosphere compared to ground-based Raman lidars at two Atmospheric Radiation Measurement (ARM) sites. Moreover, they noted that the undetected aerosols lead to underestimation of the CALIOP-inferred aerosol direct radiative effect by 30 – 50%.

Though *Rogers et al.* [2014] quantified the undetected CALIOP AOD using airborne HSRL for the North America and the Caribbean region, in this study we characterize the optical depth of the undetected aerosol on a global scale. For the purposes of this study, undetected aerosol layers include spatially diffuse aerosols that the CALIOP detection scheme routinely misses and are not limited to features with clearly defined boundaries. Both constrained and unconstrained aerosol retrievals are performed using two years (March 2013 – February 2015) of the CALIOP Level 1B data. The constrained aerosol retrieval using AOD from MODIS on the Aqua satellite is described in Section 4.1. We derive an estimated lidar ratio from the MODIS-AOD constrained retrieval and apply it where the constrained retrieval is not feasible. Since, the MODIS AOD is available only for daytime and the uncertainty over land is relatively large, we perform an unconstrained retrieval globally using the estimated lidar ratio for the undetected layers at nighttime and over land to investigate the spatio-temporal variation of the undetected CALIOP AOD in Section 4.2.

2. Data

2.1 CALIOP

The total attenuated backscatter (TAB) at 532 nm from the CALIOP Level 1B Product (Version 4) is used to retrieve aerosol extinction. The TAB is the measured lidar signal that is ranged-corrected and normalized for range-independent parameters such as laser energy, amplifier gain, and calibration constant [*Powell et al.*, 2009]. The molecular and ozone number density profiles from the NASA Global Modeling and Assimilation Office (GMAO) [*Bloom et al.*, 2005], provided as part of the CALIOP Level 1B Products, are used for molecular extinction and ozone absorption in the aerosol extinction retrieval. To determine aerosol extinction using the MODIS AOD as a constraint, we average 45 – 60 profiles of the TAB (333 m in horizontal resolution) depending on the distance between the CALIPSO ground track and MODIS grid (see section 3.1). For the retrieval with the estimated lidar ratio (Section 4.2), we average 60 profiles, i.e., 20 km in horizontal resolution. Profiles containing cloud layers are rejected using the Level 2 Cloud Layer Product (333 m, Version 3). Aerosol extinction is retrieved when 30 or more TAB profiles remain after removing cloud contamination. Before the averaging of TAB profiles, signals below the Earth's surface are removed to avoid a contamination by surface returns using the digital elevation map (DEM) surface elevation data from the CALIOP Level 1B Products. Vertical resolution for the TAB at 532 nm varies with altitude from 30 m to 300 m. We adjust this to 60 m from the surface to 20.2 km and 180 m from 20.2 km to 30.1 km to match vertical resolution of the CALIOP Level 2 Aerosol Profile Products. Though the Level 2 Aerosol Profile Product does not provide aerosol extinction above 30 km up to 35 km, aerosol extinction is retrieved with vertical resolution of 300 m from the Level 1B TAB profiles in this study. The cloud optical depth (COD) and stratospheric optical depth (SOD) at 532 nm for corresponding CALIOP Level 2 Products are used to remove TAB profiles including cloud and stratospheric features from the retrieval. For this task we use CALIOP Version 3.30 products from March 2013 to February 2015 (two years) employing the same GMAO meteorological data set of the Goddard Earth Observing System Version 5.9.1 (GEOS5) Forward Processing for Instrument Teams (FP-IT).

2.2 MODIS

MODIS is a satellite sensor onboard Terra (since 2000) and Aqua (since 2002) providing essential information on the characteristics of global aerosols [*Remer et al.*, 2008]. MODIS measures radiances in 36 channels with a wide spectral range from 0.4 μm to 14.4 μm. It has a broad swath of 2330 km and relatively fine spatial resolution (250 m to 1 km depending on band), which can provide global coverage every one to two days. Since CALIPSO and Aqua are in the 'A-Train Constellation' [*L'Ecuyer and Jiang*, 2010], they are in the same orbit with a time gap of less than 2 minutes. Therefore, CALIOP and MODIS (hereafter, MODIS refers the MODIS instrument onboard Aqua) observe aerosol optical properties of the same target nearly simultaneously.

In this study, MODIS AOD (Effective_Optical_Depth_Average_Ocean) retrievals at 550 nm from Level 2 Aerosol Products (MYD04_L2) Collection 6 [*Levy et al.*, 2013] are used as a constraint for aerosol extinction retrievals from the CALIOP TAB profiles. Because the expected uncertainty of MODIS AOD is better over ocean ($\pm 0.05\tau \pm 0.03$) than over land ($\pm 0.15\tau \pm 0.05$) [*Remer et al.*, 2005, 2008; *Levy et al.*, 2010], we used the MODIS AOD to constrain aerosol extinction only over ocean. For QA (Quality Assurance) and cloud contamination of MODIS AOD, AODs with the QA flag 'Quality_Assurance_Ocean' equal to or higher than 1 (marginal) and 'Aerosol_Cloud_Fraction' equal to zero are selected. AODs are reported at wavelengths of 532 nm and 550 nm by CALIOP and MODIS, respectively, which can lead to discrepancy in AOD of ~3% for an Ångström Exponent of 1. The Ångström Exponent for wavelengths between 0.55 and 0.86 μm (Angstrom_Exponent_1_Ocean) is used to convert 550 nm MODIS AOD to the 532 nm AOD for constraining CALIOP inversions.

3. Methodology

3.1 Collocation of CALIOP and MODIS Measurements

MODIS Level 2 Aerosol Products provide aerosol optical properties with a horizontal resolution of 10 km by 10 km near nadir, whereas the CALIOP laser has a footprint of 70 m in diameter at the surface. CALIOP provides Level 1B profiles with a horizontal resolution of 333 m and Level 2 Products of 5 km along the ground track. The following steps are applied to collocate CALIOP and MODIS data:

(1) Find a quality assured MODIS 10 km x 10 km pixel in the Level 2 Aerosol Product which lies within 5 km of the CALIPSO ground track.

(2) Identify CALIOP Level 1B TAB profiles within 10 km from the center of the MODIS pixel.

(3) Of these, discard TAB profiles which contain cloud signals using CALIOP 333-m Level 2 Cloud product.

(4) The collocated dataset consists of 30 or more cloud-free TAB profiles with a cloud optical depth (COD) and stratospheric optical depth (SOD) of zero and the MODIS pixel from (1).

Aerosol extinction is retrieved from the averaged CALIOP Level 1B collocated TAB profiles. Typically, each dataset is horizontally averaged for 16 – 20 km (48 – 60 profiles) based on the relative distance between the MODIS pixel and the CALIPSO ground track.

3.2 AOD constrained retrieval

An iterative method, similar to *Young and Vaughan* [2009], is employed to retrieve aerosol extinction. The CALIOP Level 2 algorithm retrieves aerosol extinction from top to base of the detected aerosol layer [*Young and Vaughan*, 2009; *Vaughan et al.*, 2009]. In this study, the retrieval range is extended from the detected layer top to higher altitudes up to 35 km. Retrieved aerosol extinction for undetected layers is very small and shows large fluctuations with frequent negative values because of low signal to noise ratio (SNR). The negative extinction has no physical meaning but has not been omitted to avoid bias when calculating AOD and mean extinction profiles.

The TAB $\beta'(r)$ provided by the CALIOP Level 1B Product can be written as

$$\beta'(r) = \left[\beta_m(r) + \beta_p(r)\right] T_m^2(r_0, r) T_p^2(r_0, r) T_o^2(r_0, r), \quad (1)$$

where $\beta(r)$ is the backscatter coefficient at range r from the satellite, $T^2(r_0, r)$ represents the two-way transmittance between a calibration region at r_c (36-39 km for the Version 4) and range r, and subscripts *m*, *p*, and *o* refer to molecular, particles (aerosols), and ozone, respectively. The molecular and ozone contributions in the Equation (1) are known from their vertical profiles of number density. The two-way transmittance of particles is expressed by

$$T_p^2(r_0, r) = exp\left[-2 \int_{r_0}^{r} \sigma_p(r') dr'\right], \quad (2)$$

Where $\sigma_p(r)$ is the aerosol extinction coefficient at range r. Since the Equation (1) is ill-posed with two unknowns (aerosol backscatter and extinction coefficients) in one equation, the extinction-to-backscatter ratio (lidar ratio) for aerosol, $S_p(r)$, which is defined as

$$S_p(r) = \sigma_p(r) / \beta_p(r) \quad (3)$$

is widely used to retrieve backscatter and extinction, in the so called unconstrained solution [*Fernald et al.*, 1972; *Fernald*, 1984]. If additional information is available, however, such as transmittance and AOD, the equation can be solved without assuming a lidar ratio leading to the so called constrained solution [*Young*, 1995; *Welton et al.*, 2000]. The CALIOP Level 2 retrieval algorithm uses both constrained and unconstrained retrievals using two-way transmittance and pre-determined lidar ratios for each aerosol type [*Omar et al.*, 2009; *Young and Vaughan*, 2009].

The retrieval method using MODIS AOD as a constraint in this study is similar to the approach described in *Burton et al.* [2010]. An analogous technique for ground-based lidar measurements uses AODs from Sun photometers [e.g., *Welton et al.*, 2000; *Voss et al.*, 2001; *Murayama et al.*, 2003]. A flowchart for the retrieval is shown in Figure 1. The collocated dataset includes MODIS (AOD, QA, cloud fraction, and Ångström Exponent) and CALIOP (TAB, molecular and ozone number density, aerosol layer top and base altitudes, COD, SOD, and surface elevation). Using an initial lidar ratio (S_0), we retrieve aerosol extinction coefficients. After retrieving aerosol extinction profile (σ_p), the CALIOP AOD (τ_{CAL}) is calculated by vertical integration of the retrieved aerosol extinction coefficients. The aerosol lidar ratio (S_p) is then adjusted by comparing the AOD from CALIOP (τ_{CAL}) with MODIS (τ_{MOD}). The iterative retrieval ends when the difference of AOD between CALIOP and MODIS, ε, becomes less than 1%. For the vertical integration of aerosol extinction, the lower limit (sfc) is 120 m above the surface to ensure that the averaged TAB profiles exclude surface returns, and the upper limit (top) is extended from top of the detected layers up to 35 km above mean sea level. The bias in the undetected layer AOD (ULA) introduced by ignoring the aerosol in the lowest 120 m of the atmosphere is negligible (less than 1%). For the purposes of this study, the lidar ratio is assumed constant in the atmospheric column (e.g., as in *Burton et al*. [2010] and *Dawson et al*. [2015]).

We hypothesize that there are undetected aerosol layers above and between the detected aerosol layers and regions where CALIOP finds no layers (CALIOP AOD = 0). Since CALIOP AOD is calculated only from the detected layers, the CALIOP AOD is smaller than the total column AOD. Further, we hypothesize that the AOD retrieved including clear regions will be closer to the total column AOD as we increase the range above the detected layer. This will be tested by incrementally increasing top height of the column from 5 km to 35 km, and noting the retrieved column AOD and lidar ratios. Since the CALIOP Level 1B (Version 4) Products are normalized to the molecular signal at 36 – 39 km, the initial altitude for the retrieval cannot be extended higher than this range. In order to investigate the ULA from the CALIOP Level 2 algorithm, aerosol extinction profiles retrieved in this study are integrated by excluding layers where the vertical feature mask (VFM) from CALIOP Level 2 Profile Product reports an aerosol layer.

3.3 Unconstrained retrieval

The MODIS AOD constrained retrieval is possible only at daytime. Moreover, the retrieval is limited to the ocean in this study because of the large uncertainty in MODIS AOD over land. In order to extend the retrieval to land and at nighttime, the unconstrained retrieval is applied using an estimated lidar ratio for the undetected layers determined from a distribution of the constrained retrievals. Collocated datasets of clean cases where CALIOP detects only marine boundary layer are chosen to estimate lidar ratio for the undetected layers. Because the lidar ratio for clean marine aerosol is well known, we can fix the lidar ratio for marine boundary layer at 23 sr [*Burton et al., 2013*; *Rogers et al., 2014*]. Thus, the lidar ratio for undetected layers can be determined from the AOD constrained retrieval (Figure 1) by fixing the lidar ratio for clean marine aerosol and adjusting lidar ratio only for the undetected layers. Note that all results in Section 4.2 are from the unconstrained retrieval using the estimated lidar ratio and TAB only.

4. Results

4.1 Retrieval using MODIS AOD as a constraint

The CALIOP Level 2 algorithm retrieves aerosol extinction only for detected layers whereas MODIS AOD is for the whole atmospheric column from the top of the atmosphere (TOA) to the surface. Thus, aerosol extinction retrievals from higher altitudes are more accurate when using MODIS AOD as a constraint because they are more inclusive of the undetected features. In this study, the extinction is retrieved from the CALIOP Level 1B Product using initial top altitudes of 35 km, 25 km, 15 km, 5 km and top of the detected layer as shown in Figure 2 for March 2013 to February 2015. The retrieved lidar ratio distributions are shown in Figure 3. For aerosol extinction retrieved from the top of the detected layer to the surface using MODIS AOD as a constraint (Figure 3e), the lidar ratios are large with the mean of 57.32 sr. This is because the MODIS AOD is larger than CALIOP AOD for most of the dataset as reported by many previous studies [e.g., *Oo and Holz,* 2011; *Redemann et al.*, 2012; *Kim et al.*, 2013]. The larger lidar ratio compensates for the missing AOD from CALIOP. As the initial altitude for the retrieval (hereafter referred to as the initial altitude) is increased, the lidar ratio decreases, an indication that as more undetected layers are accounted for, the column lidar ratio is closer to truth and the distribution is narrower.

Table 1 shows mean AODs for MODIS, CALIOP, and retrieved in this study for the detected and undetected layers from different initial altitudes from March 2013 to February 2015. In Table 1, the total retrieved AOD (sum of detected and undetected) always equals to MODIS AOD which is used as constraint. The CALIOP AOD corresponds to the AOD for detected layers, but has different values because the lidar ratios used in the retrievals are different. As shown in Figure 3, lidar ratio decreases as the initial altitude increases, which results in decrease of retrieved AOD for the detected layers. On the other hand, since more undetected layers are included, ULA increases as the initial altitude increases. The values in Table 1 are only for successful retrievals and might be different from mean AODs for CALIOP and MODIS reported by previous studies. Here, the success rate in Table 1 represents successful retrievals out of total retrieval attempts. The retrieval sometimes diverges and fails to find solution, which leads to “failed” retrievals.

The global mean profiles of total retrieved extinction for different initial altitudes are shown in Figure 4. In the free atmosphere, aerosol extinction is small when the initial altitude is low. Because AOD above the initial altitude is assumed to be zero, the two-way transmittance of aerosol from the calibration altitude to the initial altitude is overestimated in Equation 1 when the initial altitude is low, which leads to small aerosol extinction. However, aerosol extinction increases rapidly with decrease of altitude for low initial altitudes due to larger lidar ratios. For this reason, when the initial altitude for AOD constrained retrieval is not high enough, aerosol extinction is underestimated for the free atmosphere but overestimated for the low atmosphere near the surface.

The lidar ratios obtained from the AOD constrained retrieval are averaged values for whole atmospheric column including both detected and undetected layers. The ULA shown in Table 1 thus increases or decreases based on changes in lidar ratio for the undetected layers. A global mean lidar ratio for undetected layers is estimated from the AOD constrained retrieval using the method described in Section 3.3. The mean (± standard deviation) and median (± median absolute deviation) lidar ratio for undetected layers retrieved from these samples are 32.62 ± 18.62 sr and 28.75 ± 10.29 sr, respectively (Figure 5). Since the distribution is highly skewed and has a large standard deviation, the median is used as the representative lidar ratio for the undetected layers. We assume that the undetected layers are mostly dominated by clean background aerosols and spatio-temporal variation of the lidar ratio for the undetected layers is negligible.

4.2 Unconstrained retrieval for the undetected layer AOD

Figure 5 shows the distribution of lidar ratios of undetected layers retrieved using the procedure described in section 3.3. Using the median value of 28.75 sr for the undetected aerosol layers, aerosol extinction is retrieved from the CALIOP Level 1B Product from 35 km to the surface for both day and night, over land and ocean. We use the lidar ratios reported in the CALIOP Level 2 Product for the detected layers. The mean AODs for detected (CALIOP Level 2 Products) and undetected layers (retrieved in this study) from the unconstrained retrieval are summarized in Table 2. The global mean ULA is 0.031 ± 0.052. The total retrieved AOD and corresponding CALIOP AOD are 0.116 ± 0.149 and 0.070 ± 0.123, respectively. The summation of AOD for detected (CALIOP) and undetected layers should equal to whole column AOD in Table 1. However, the CALIOP AOD is different from the AOD for detected layers retrieved in this study because of the difference in horizontal and vertical averaging and the correction for the two-way transmittance above the layer that is applied in this study but not in the CALIOP Level 2 retrieval algorithm. An overestimation of the two-way transmittance of aerosol by assuming no aerosol above the detected layers for the CALIOP Level 2 retrieval leads to low CALIOP AOD compared with AOD retrieved in this study [*Young et al.*, 2013].

Compared to the constrained retrieval results, the mean AODs for the sum of detected and undetected layers are smaller for unconstrained retrievals. This is primarily a sampling issue. The smaller CALIOP AOD for the unconstrained retrieval is mainly due to the inclusion of low AODs retrieved over snow-covered regions in high latitudes, especially in Polar Regions. Because MODIS rarely retrieves AOD with high confidence over bright surfaces, many records with low AOD over those regions are excluded for the constrained retrieval. Smaller mean ULA for the unconstrained retrieval is caused by differences in the lidar ratio. The (mean ± standard deviation) lidar ratio for constrained retrieval (31.75 ± 12.26 sr) are determined by MODIS AOD as shown in Figure 3(a), whereas a median lidar ratio of 28.75 sr (Figure 5) determined from a constrained retrieval of all layers above the marine boundary layer (MBL), is used for unconstrained retrieval. The ULA is close to the mean bias range between 0.03 and 0.04 from *Redemann et al*. [2012] and comparable with other studies; mean AOD bias of 0.043 between CALIOP and MODIS reported by *Kim et al*. [2013], and mean bias of 0.064 from *Oo and Holz* [2011]. This implies that a major reason for the underestimation of AOD by CALIOP when compared to MODIS AOD is due to the undetected layers by the CALIOP Level 2 layer detection algorithm.

4.2.1 Undetected layer AOD – day vs. night

The ULA during day and night varies significantly in both its mean and standard deviation (Table 1, Figure 6a, 6b). The broader distribution in Figure 6(a) arises from the lower SNR in the CALIOP measurements during daytime compared to nighttime. The mean ULA for daytime (0.036 ± 0.066) is ~44% larger than nighttime (0.025 ± 0.021). Our nighttime ULA estimate is slightly larger than the value of ~0.02 reported by *Rogers et al.* [2014]. This is not unexpected, as in this study we use CALIOP data to retrieve aerosol extinction over the globe up to an altitude of 35 km, whereas the Rogers et al. estimate is derived from HSRL measurements acquired only in North America and the Caribbean, and their AOD integration height was limited to ~7.5 km (i.e., the aircraft flight altitude). Another difference between the two studies is that we specifically include those CALIOP profiles in which no aerosols were detected (i.e., AOD = 0) in cloud-free skies. While excluding these data is of little consequence within the limited temporal and spatial domain considered by *Rogers et al.* [2014], when examining data on a global scale, we find that the CALIOP Level 2 layer detection algorithm fails to identify aerosols in 17–20% of the cases where we subsequently retrieved aerosol extinction in the 30°N–40°N latitude band (i.e., in the same general region as many of the *Rogers et al.* [2014] measurements). While the *Rogers et al.* [2014] study concludes that for nighttime measurements the AOD from missing layers is insignificant compared with errors in the CALIOP AOD arising from other sources, our results suggest instead that ULA during nighttime (0.025) is not negligible when compared with the corresponding mean AOD (0.074) reported in the CALIOP version 3 data products. During daytime, *Rogers et al*. [2014] find that CALIOP fails to detect aerosols in roughly half of the profiles in which HSRL measures and AOD less than 0.1. Our results are similar. Our analyses show that CALIOP detects only 60% of total AOD during daytime. CALIOP's detection efficiency is much better at night than during, and hence the daytime ULA (0.036) is much larger than the nighttime value.

Vertical profiles of aerosol extinction for undetected layers for day and night are shown in Figure 6(c) along with aerosol extinction profiles from the CALIOP Level 2 Profile Products which represent the extinction for detected layers. CALIOP detects a higher AOD during nighttime at altitudes above 1 km. Aerosol extinction below 1 km, on the other hand, is larger during daytime than nighttime probably due to enhanced generation of anthropogenic aerosols during daytime over land [*Smirnov et al.*, 2002]. Unlike extinction profiles for detected layers, undetected aerosol extinction for daytime is larger than nighttime not only near the surface but also in the upper atmosphere. The total attenuated backscatter from the CALIOP Level 1B Products is noisier during daytime than nighttime and more likely to confound detection of tenuous aerosol layers in the CALIOP layer detection algorithm [*Vaughan et al.*, 2009]. *Winker et al.* [2013] showed that the detection thresholds used in the CALIOP Level 2 data processing is much larger for daytime than nighttime. *Rogers et al.* [2014] reported similar estimation of the minimum extinction detection threshold for CALIOP; 0.012 km^{-1} for nighttime and 0.067 km^{-1} for daytime.

4.2.2 Undetected layer AOD – land vs. ocean

The ULA over land (0.033 ± 0.059) is ~10% larger than over ocean (0.030 ± 0.046), but similar within the error bars. The histograms show similar probability distributions of AOD (Table 2, Figure 7a, 7b). However, the vertical distributions of the extinction over land and ocean are different (Figure 7c). The undetected aerosols are more frequently elevated to higher altitudes over land than over ocean. The extinction profile over land with the ordinate of above ground level (AGL) instead of above mean sea level (AMSL), is similar to the ocean profile above 1.5 km. Aerosols can be elevated to higher altitude (AMSL) over land than ocean because of geographical effects. A significant difference in the aerosol extinction between land and ocean appears near the surface. Since aerosols in the boundary layer are well detected, the undetected aerosol extinction decreases near the surface over ocean. On the other hand, large undetected extinction below 1.5 km AGL over land indicates that aerosols near the land surface are more frequently undetected.

Figure 6(c) and Figure 7(c) show that the aerosol extinction for undetected layers decreases exponentially with altitude. The global mean undetected aerosol extinction is ~0.002 km^{-1} at 5 km and ~0.001 km^{-1} at 10 km, which is consistent with previous reports for "background" aerosol extinction. *Kent et al.* [1998] found the mean extinction for typical background aerosols of 0.0034 km^{-1} at 532 nm from LITE measurements in the southern hemisphere (between 5°S and 45°S) from 6 km to the tropopause. *Winker et al.* [2013] report that the average lower limit on aerosol extinction between 6 km and 9 km is about 0.001 km^{-1} at 525 nm using Stratospheric Aerosol and

Gas Experiment (SAGE II) satellite data. *Winker et al.* [2013] also retrieved the aerosol extinction for whole column from the CALIOP data starting at 12 km to the surface using a constant aerosol lidar ratio. They report that the CALIOP Level 3 (monthly mean) profiles generally underestimate free tropospheric aerosol loading in clean conditions but no more than about 0.003 km^{-1}. The underestimation of CALIOP aerosol extinction corresponds to the undetected aerosol extinction shown in this study.

4.2.3 Undetected layer AOD – spatial distribution

Global distributions of the ULA show a significant difference in magnitude between day and night (Figure 8). The plots show several features of the global distribution of ULA; (1) similar in pattern between day and night, (2) high in the Northern Hemisphere, (3) relatively high over land and outflow of major aerosol source regions (especially for smoke) at mid and low latitudes, (4) low over elevated land surfaces, (5) high at high latitudes.

Figure 9 shows zonal mean aerosol extinctions for (a) total, (b) detected and (c) undetected layers. Figure 9(a) and Figure 9(b) show that the major structure of aerosols is well captured by CALIOP Level 2 layer detection algorithm and the most of aerosols are concentrated near the surface and maximum extinction appears below 1 km AMSL. On the other hand, the maximum undetected extinction (Figure 9c) is located 1 – 2 km AMSL and decreases near the surface at mid and low latitudes (60ºS - 60ºN). This implies that aerosols near the surface (PBL) are relatively well detected but aerosols near the top of the PBL and in the free troposphere are more frequently undetected. Figure 10 shows aerosol extinction profiles for total and undetected layers along with relative frequency for the undetected layers averaged for 60ºS - 60ºN. The total extinction decreases with altitude whereas the relative frequency of the undetected layers increases. Since the undetected extinction profile can be represented as a product of the total extinction and the relative frequency of undetected layers, the maximum altitude for the undetected extinction is located near 1.5 km. An interesting feature is found in Figure 9(c) around 20 km in altitude over the tropics. Stratosphere-troposphere exchange (STE) and dehydration are the main mechanisms for transport of aerosol to the stratosphere [Wang et al., 1996]. For example, overshooting clouds associated with deep convective system can transport tropospheric aerosols to the stratosphere. The results shown in this study are from the undetected or background aerosols excluding detected aerosols such as volcanic aerosols and polar stratospheric aerosols (PSAs) and are therefore representative of weak features only.

Though the total extinction is very small in Figure 9(a), the maximum undetected extinction occurs in Polar Regions (Small extinction values below 3 km AMSL in the Antarctic region are due to the surface elevation of Antarctica.). Figure 11(a) shows distributions of zonal mean AODs for total retrieved and undetected layers and CALIOP Level 2 Products which correspond to detected layers. The CALIOP AOD is smaller than the total retrieved AOD by 0.046 on average, but general features of the maximum around 10ºN, minor peak at 50ºS and low AOD at high latitudes are consistent with previous work of modeling and observations [e.g., *Myhre et al.*, 2007; *Toth et al.*, 2013; *Lacagnina et al.*, 2015]. The ULA, which corresponds to a vertical integration of Figure 9(c), does not show significant variation due to latitude. The ULA is relatively small from 50ºS to 30ºN and somewhat larger for the northern hemisphere and the Polar Regions. Figure 11(b) shows the ratio of ULA to total AOD and the ratio of cases where the CALIOP detects no aerosol layers (AOD = 0) to the whole data for cloud-free conditions. This zero-AOD for CALIOP represents cases where the CALIPO Level 2 layer detection algorithm does not detect aerosols even in the PBL. This accounts for large fraction of ULA over the Polar Regions near the surface.

4.2.4 Source of uncertainty in ULA

For this study, the signal-to-noise ratio (SNR) of the CALIOP signal at any altitude region is defined as μ/σ, where μ is the mean signal and σ is the standard deviation. Low SNR for undetected layers introduces an uncertainty and bias in the retrieval. *Young et al*. [2013] point out that the retrievals are positive-biased for low SNR (less than or equal to 1) and the bias increases with decreasing SNR. At single shot resolution, the SNR of the CALIOP Level 1B TAB is substantially less than 1 throughout the entire profile, and thus can introduce a positive bias into the retrieved AOD. To minimize this effect, TAB profiles are averaged to 20 km in horizontal and smoothed vertically with a sliding window of 300 m – 1500 m (varies with altitude) before the retrieval. The typical SNR in this study is 0.5 – 1 for day and 1 – 2 for night at around 35 km where the retrieval is initiated, which can lead to a slight positive bias in ULA.

The aerosol backscatter and extinction from the renormalization altitude to the surface can be solved from Equation (1) rewritten as

$$\beta_p(r) = \beta'_N(r)/\left[T_m^2(r_N,r)T_p^2(r_N,r)T_o^2(r_N,r)\right] - \beta_m(r), \quad (4)$$

where $T_p^2(r_N,r) = exp\left[-2\int_{r_N}^{r} S_p\,\beta_p(r)(r')dr'\right]$ and $r_N$is the altitude where the retrieval is initiated [*Young and Vaughan*, 2009; *Young et al*., 2013]. $\beta'_N(r)$ is renormalized attenuated backscatter defined as

$$\beta'_N(r) = \beta'(r)/\left[T_m^2(r_0,r_N)T_p^2(r_0,r_N)T_o^2(r_0,r_N)\right]$$

$$= [\beta_m(r) + \beta_p(r)] T_m^2(r_N, r) T_p^2(r_N, r) T_o^2(r_N, r) \; . \quad (5)$$

Since r_N (= 35 km) for unconstrained retrieval in this study is very close to r_0 which is determined between 36 – 39 km, error in the renormalization is not significant. Thus, major sources of error in ULA for the unconstrained retrieval are calibration factor and lidar ratio in Equation (4). The uncertainty in the calibration factor includes uncertainties in the molecular backscatter and two-way transmittance, and the estimated scattering ratio at the calibration range [*Young et al.*, 2013]. The uncertainty in the lidar ratio corresponds to the errors in the constrained retrieval because it is determined from the constrained retrieval using MODIS AOD as a constraint. Assuming the lidar ratio is constant without spatio-temporal variability for undetected layers also introduces uncertainty in the extinction retrieval [*Burton et al.*, 2010].

Figure 12 shows simple sensitivity tests with respect to the calibration factor and the lidar ratio. ULA is very sensitive to both calibration factor and lidar ratio. Using comparisons with collocated airborne HSRL measurements, Rogers et al. [2011] estimate calibration coefficient uncertainties for the Version 3 CALIOP Level 1B Products as 2.7% ± 2.1% at night and 2.9% ± 3.9% during daytime, with the CALIOP attenuated backscatter coefficients being biased low relative to the HSRL measurements (i.e., the V3 CALIOP calibration coefficients are biased high). Vernier et al. (2009) estimate that CALIOP level 1B Version 3 TAB is systematically biased low by 2% to as much as 10%, depending on latitude and season, due to unacknowledged aerosol loading in the Version 3 calibration region between 30 – 34 km. They suggest calibrating in the relatively aerosol-free region of 36–39 km identified in both SAGE and CALIOP data. This suggestion is implemented in CALIOP data processing for Version 4 Product which is used in this study [Getzewich et al., 2016]. Calibration biases relative to the HSRL data set are now reduced to 0.2% ± 2.4% at night and -0.2% ± 3.9% during daytime [*Toth et al.*, 2106]. Figure 12(a) shows that the error of 5% in the calibration results in large ULA bias (-57%), but relatively small bias in ULA (2.5%) for the calibration error of 0.2%.

Uncertainty in ULA due to error in the lidar ratio is more significant. *Voss et al.* [2001] found the lidar ratio of 32 ± 6 sr for the clean Northern Hemisphere aerosol measured during the Aerosols99 cruise. *Ansmann et al.* [2001] report the lidar ratios around 35 sr for background-like aerosol during the Second Aerosol Characterization Experiment (ACE 2). Similarly, CALIPSO Version 3 algorithm uses the lidar ratio of 35 sr for clean background (clean continental) aerosol [*Omar et al.*, 2009]. Larger lidar ratios for the background aerosols are used by *Heese and Wiegner* [2008] (55 sr) and *Immler and Schrems* [2003] (44 ± 5 sr), whereas *Tesche et al.* [2007] found unexpectedly low lidar ratios of approximately 25 sr for a case of background aerosol with a low optical depth of 0.05 from Raman lidar in China. The mean (32.62 ± 18.62 sr) and median (28.75 ± 10.29 sr) lidar ratio for undetected layers retrieved in this study is slightly smaller than these values. However, the lidar ratio for undetected layers estimated in this study includes not only background aerosols but also undetected aerosols of various types. Moreover, optical properties of background aerosols in the upper troposphere and stratosphere can be different from those in the low troposphere. *Kent et al.* [1998] shows that the lidar ratio in the stratosphere and upper stratosphere lies in the relatively broad range 20 – 50 sr at 532 nm from Mie calculations for aerosols from biogenic, anthropogenic or volcanic sources. An error of 10 sr in the lidar ratio leads to ~50% in ULA when the lidar ratio for undetected layer is about 30 sr. However, ULA increases rapidly for lidar ratios larger than 40 sr (Figure 12b).

5. Conclusions

Aerosol extinction is retrieved from the total attenuated backscatter at 532 nm of CALIOP Level 1B Products, without an *a priori* assumption of an aerosol lidar ratio, using collocated MODIS AOD as a constraint at daytime over ocean. We found that the retrieved lidar ratio depends on the altitude at which the retrieval is initiated implying that the AOD from undetected layers above the aerosol layers reported in the CALIOP Level 2 products is not negligible and can affect the column-averaged lidar ratio and AOD. In this study, the lidar ratio for undetected layers is estimated using distributions from the AOD constrained method, and applied to all undetected layers including nighttime and over land. Major findings are as follows.

- The global mean (± standard deviation) and median (± median absolute deviation) aerosol lidar ratio for the undetected layers are 32.62 ± 18.62 sr and 28.75 ± 10.29 sr, respectively, from CALIOP Level 1B Products using MODIS AOD as a constraint. From an unconstrained retrieval using the estimated lidar ratio (28.75 sr), the global mean AOD for the undetected layers in CALIOP Level 2 Products is 0.031 ± 0.052 which corresponds to 25.9% of mean total retrieved AOD and 44.3% of mean CALIOP AOD. This result depends on the accuracy of the estimated lidar ratio value of 28.75 sr.

- ULA values are similar within the error bars between land (0.033 ± 0.059) and ocean (0.030 ± 0.046). Aerosols near the surface are less frequently detected by the CALIOP layer detection algorithm over land.

- Whereas the total AOD for daytime (0.113 ± 0.150) is only 6% smaller than nighttime (0.120 ± 0.149), ULA shows a large difference between day (0.036 ± 0.066) and night (0.025 ± 0.021). The increase in undetected layers during daytime is likely due to lower SNR at daytime.

- ULA is small near the surface but has maximum at 1 – 2 km AMSL for mid and low latitudes (60ºS - 60ºN). This implies that aerosols in the PBL are relatively well detected but aerosols near the top of the boundary layer are more frequently undetected.

- ULA is larger in the northern hemisphere than the southern hemisphere and has minimum at 40ºS and maximum in the Arctic. Large ULA for the Polar Regions is strongly related to the cases where CALIOP reports zero AOD. Due to low SNR, CALIOP does not detect aerosol layers in Polar Regions in more than 60% of cloud free opportunities.

This study provides an estimate of the complement of AOD that is not detected by lidar to bound CALIOP AOD uncertainty and provide corrections for studies that employ the CALIOP Level 2 AOD. The ULA retrieved in this study includes AODs not only from layers not detected by the CALIOP Level 2 layer detection algorithm but also from weak background aerosols. These can be reduced by improving the detection capability of the algorithms and increasing the SNR, e.g., by increasing spatial averaging to 160 or 240 km. However, the ULA cannot be completely accounted for unless the CALIOP Level 2 algorithm retrieves whole atmospheric column. It is challenging to adapt a whole-column retrieval in CALIOP Level 2 algorithm because of the low SNR for the undetected layers. As shown in Figure 6 and Figure 7, the ULA ranges from -0.1 to values above +0.2.

Acknowledgements

The CALIPSO data used in this study were obtained from the NASA Langley Atmospheric Science Data Center. The MODIS data were obtained through the NASA Goddard Space and Flight Center Data Center. Man-Hae Kim was supported by a NASA Postdoctoral Program Fellowship. Sang-Woo Kim was supported by the KMA R&D program under Grant KMIPA 2015-2011.

References

Andersson, S. M., B. G. Martinsson, J. P. Vernier, J. Friberg, C. A. M. Brenninkmeijer, M. Hermann, P. van Velthoven and A. Zahn (2015), Significant radiative impact of volcanic aerosol in the lowermost stratosphere, *Nature Communications*, 6, 7692, doi:10.1038/ncomms8692.

Ansmann, A., F. Wagner, D. Althausen, D. Müller, A. Herber, and U. Wandinger (2001), European pollution outbreaks during ACE 2: Lofted aerosol plumes observed with Raman lidar at the Portuguese coast, *J. Geophys. Res.*, 106(D18), 20725–20733, doi:10.1029/2000JD000091.

Bloom, S., and Coauthors (2005), Documentation and validation of the Goddard Earth Observing System (GEOS) data assimilation system—Version 4. Tech. Rep. Series on Global Modeling and Data Assimilation, NASA/TM-2005-104606, Vol. 26, 165 pp.

Bösenberg, J., et al. (2003), EARLINET: A European Aerosol Research Lidar Network to establish an aerosol climatology, *Report No. 348*, Max Plank Institute for Meteorolgy, Hamburg, Germany.

Burton, S. P., R. A. Ferrare, C. A. Hostetler, J. W. Hair, C. Kittaka, M. A. Vaughan, M. D. Obland, R. R. Rogers, A. L. Cook, D. B. Harper, and L. A. Remer (2010), Using airborne high spectral resolution lidar data to evaluate combined active plus passive retrievals of aerosol extinction profiles, *J. Geophys. Res.*, 115, D00H15, doi:10.1029/2009JD012130.

Burton, S. P., R. A. Ferrare, M. A. Vaughan, A. H. Omar, R. R. Rogers, C. A. Hostetler, and J. W. Hair (2013), Aerosol classification from airborne HSRL and comparisons with the

CALIPSO vertical feature mask, *Atmos. Meas. Tech.*, 6, 1397–1412, doi:10.5194/amt-6-1397-2013.

Chand, D., R. Wood, T. L. Anderson, S. K. Satheesh, and R. J. Charlson (2009), Satellite-derived direct radiative effect of aerosols dependent on cloud cover, *Nat. Geosci.*, 2, 181–184, doi:10.1038/ngeo437.

Dawson, K. W., N. Meskhidze, D. Josset, and S. Gassó (2015), Spaceborne observations of the lidar ratio of marine aerosols, *Atmos. Chem. Phys.*, 15, 3241-3255, doi:10.5194/acp-15-3241-2015.

Fernald, F. G. (1984), Analysis of atmospheric lidar observations: Some comments, *App. Opt.*, 23, 652–653.

Fernald, F. G., B. M. Herman and J. A. Reagan (1972), Determination of aerosol height distributions by lidar, *J. Appl. Meteorol.*, 11, 482–489.

Getzewich, B. J., J. L. Tackett, J. Kar, A. Garnier, M. A. Vaughan and B. Hunt (2016), CALIOP Calibration: Version 4.0 Algorithm Updates, *EPJ Web of Conferences*, 119, 04013, doi:10.1051/epjconf/201611904013.

Heese, B., and M. Wiegner (2008), Vertical aerosol profiles from Raman polarization lidar observations during the dry season AMMA field campaign, *J. Geophys. Res.*, 113, D00C11, doi:10.1029/2007JD009487.

Huang, J., P. Minnis, B. Chen, Z. Huang, Z. Liu, Q. Zhao, Y. Yi, and J. K. Ayers (2008), Long-range transport and vertical structure of Asian dust from CALIPSO and surface measurements during PACDEX, *J. Geophys. Res.*, 113, D23212, doi:10.1029/2008JD010620.

Huang, J., Q. Fu, J. Su, Q. Tang, P. Minnis, Y. Hu, Y. Yi, and Q. Zhao (2009), Taklimakan dust aerosol radiative heating derived from CALIPSO observations using the Fu-Liou radiation model with CERES constraints, *Atmos. Chem. Phys.*, 9, 4011-4021, doi:10.5194/acp-9-4011-2009.

Immler, F. and O. Schrems (2003), Vertical profiles, optical and microphysical properties of Saharan dust layers determined by a ship-borne lidar, *Atmos. Chem. Phys.*, 3, 1353-1364, doi:10.5194/acp-3-1353-2003.

Kacenelenbogen, M., M. A. Vaughan, J. Redemann, R. M. Hoff, R. R. Rogers, R. A. Ferrare, P. B. Russell, C. A. Hostetler, J. W. Hair, and B. N. Holben (2011), An accuracy assessment of the CALIOP/CALIPSO version 2/version 3 daytime aerosol extinction product based on a detailed multi-sensor, multi-platform case study, *Atmos. Chem. Phys.*, 11, 3981-4000, doi:10.5194/acp-11-3981-2011.

Kacenelenbogen, M., J. Redemann, M. A. Vaughan, A. H. Omar, P. B. Russell, S. Burton, R. R. Rogers, R. A. Ferrare, and C. A. Hostetler (2014), An evaluation of CALIOP/CALIPSO's aerosol-above-cloud detection and retrieval capability over North America, *J. Geophys. Res. Atmos.*, 119, 230–244, doi:10.1002/2013JD020178.

Kent, G. S., C. R. Trepte, K. M. Skeens, and D. M. Winker (1998), LITE and SAGE II measurements of aerosols in the southern hemisphere upper troposphere, *J. Geophys. Res.*, 103(D15), 19111–19127, doi:10.1029/98JD00364.

Kim, D., M. Chin, H. Yu, T. Diehl, Q. Tan, R. A. Kahn, K. Tsigaridis, S. E. Bauer, T. Takemura, L. Pozzoli, N. Bellouin, M. Schulz, S. Peyridieu, A. Chédin and B. Koffi (2014), Sources, sinks, and transatlantic transport of North African dust aerosol: A multimodel analysis and comparison with remote sensing data, *J. Geophys. Res. Atmos.*, 119, 6259–6277, doi:10.1002/2013JD021099.

Kim, M.-H., S.-W. Kim, S.-C. Yoon, and A. H. Omar (2013), Comparison of aerosol optical depth between CALIOP and MODIS-Aqua forCALIOP aerosol subtypes over the ocean, *J. Geophys. Res.Atmos.*, 118, 13,241–13,252, doi:10.1002/2013JD019527.

Kim, S.-W., S. Berthier, P. Chazette, J.-C. Raut, F. Dulac, and S.-C. Yoon (2008), Validation of aerosol and cloud layer structures from the space-borne lidar CALIOP using Seoul National University ground-based lidar, *Atmos. Chem. Phys.*, 8, 3705-3720, doi:10.5194/acp-8-3705-2008.

Kittaka, C., D. M. Winker, M. A. Vaughan, A. Omar, and L. A. Remer (2011) Intercomparison of column aerosol optical depths from CALIPSO and MODIS-Aqua, *Atmos. Meas. Tech.*, 4, 131-141, doi:10.5194/amt-4-131-2011.

Koffi, B. et al. (2012), Application of the CALIOP Layer Product to evaluate the vertical distribution of aerosols estimated by global models: Part 1. AeroCom phase I results, *J. Geophys. Res.*, 117, D10201, doi:10.1029/2011JD016858.

L'Ecuyer, T. S., and J. H. Jiang (2010), Touring the atmosphere aboard the A-Train, *Phys. Today*, 63(7), 36–41, doi:10.1063/1.3463626.

Lacagnina, C., O. P. Hasekamp, H. Bian, G. Curci, G. Myhre, T. van Noije, M. Schulz, R. B. Skeie, T. Takemura, and K. Zhang (2015), Aerosol single-scattering albedo over the global oceans: Comparing PARASOL retrievals with AERONET, OMI, and AeroCom models estimates, *J. Geophys. Res.*, 120, 9814–9836, doi:10.1002/2015JD023501.

Levy, R. C., L. A. Remer, R. G. Kleidman, S. Mattoo, C. Ichoku, R. Kahn, and T. F. Eck (2010), Global evaluation of the Collection 5 MODIS dark-target aerosol products over land, *Atmos. Chem. Phys.*, 10, 10399–10420, doi:10.5194/acp-10-10399-2010.

Levy, R. C., S. Mattoo, L. A. Munchak, L. A. Remer, A. M. Sayer, F. Patadia, and N. C. Hsu (2013), The Collection 6 MODIS aerosol products over land and ocean, *Atmos. Meas. Tech.*, 6, 2989-3034, doi:10.5194/amt-6-2989-2013.

Liu, Z., A. Omar, M. Vaughan, J. Hair, C. Kittaka, Y. Hu, K. Powell, C. Trepte, D. Winker, C. Hostetler, R. Ferrare, and R. Pierce (2008), CALIPSO lidar observations of the optical properties of Saharan dust: A case study of long-range transport, *J. Geophys. Res.*, 113, D07207, doi:10.1029/2007JD008878.

Liu, Z., D. Winker, A. Omar, M. Vaughan, J. Kar, C. Trepte, Y. Hu, and G. Schuster (2015), Evaluation of CALIOP 532 nm aerosol optical depth over opaque water clouds, *Atmos. Chem. Phys.*, 15, 1265-1288, doi:10.5194/acp-15-1265-2015.

Mamouri, R. E., V. Amiridis, A. Papayannis, E. Giannakaki, G. Tsaknakis, and D. S. Balis (2009), Validation of CALIPSO space-borne-derived attenuated backscatter coefficient profiles using a ground-based lidar in Athens, Greece, *Atmos. Meas. Tech.*, 2, 513-522, doi:10.5194/amt-2-513-2009.

Matus, A. V., T. S. L'Ecuyer, J. E. Kay, C. Hannay and J.-F. Lamarque (2015), The Role of Clouds in Modulating Global Aerosol Direct Radiative Effects in Spaceborne Active Observations and the Community Earth System Model, *J. Climate*, 28, 2986-3003, doi:10.1175/JCLI-D-14-00426.1.

McGill, M. J., M. A. Vaughan, C. R. Trepte, W. D. Hart, D. L. Hlavka, D. M. Winker, and R. Kuehn (2007), Airborne validation of spatial properties measured by the CALIPSO lidar, *J. Geophys. Res.*, 112, D20201, doi:10.1029/2007JD008768.

Mona, L., A. Amodeo, A. Boselli, G. D´Amico, A. Giunta, F. Madonna, F. Russo, and G. Pappalardo (2009), One year of CNR-IMAA multi-wavelength Raman lidar measurements in correspondence of CALIPSO overpass: Level 1B products comparison, *Atmos. Chem. Phys.*, 9, 7213-7228, doi: 10.5194/acpd-9-8429-2009.

Murayama, T., et al. (2003), An intercomparison of lidar-derived aerosol optical properties with airborne measurements near Tokyo during ACE-Asia, *J. Geophys. Res.*, 108(D23), 8651, doi:10.1029/2002JD003259.

Myhre, G., N. Bellouin, T. F. Berglen, T. K. Berntsen, O. Boucher, A. Grini, I. S. A. Isaksen, M. Johnsrud, M. I. Mishchenko, F. Stordal, and D. Tanré (2007), Comparison of the radiative properties and direct radiative effect of aerosols from a global aerosol model and remote sensing data over ocean, *Tellus B*, 59, 115–129, doi: 10.1111/j.1600-0889.2006.00226.x.

Oikawa, E., T. Nakajima, T. Inoue and D. Winker (2013), A study of the shortwave direct aerosol forcing using ESSP/CALIPSO observation and GCM simulation, *J. Geophys. Res.*, 118, 3687-3708, doi:10.1002/jgrd.50227.

Omar, A. H., D. M. Winker, J. L. Tackett, D. M. Giles, J. Kar, Z. Liu, M. A. Vaughan, K. A. Powell, and C. R. Trepte (2013), CALIOP and AERONET aerosol optical depth comparisons: One size fits none, *J. Geophys. Res.*, 118, 1–19, doi:10.1002/jgrd.50330.

Omar, A., D. Winker, C. Kittaka, M. Vaughan, Z. Liu, Y. Hu, C. Trepte, R. Rogers, R. Ferrare, R. Kuehn, C. Hostetler (2009), The CALIPSO Automated Aerosol Classification and Lidar Ratio Selection Algorithm, *J. Atmos. Oceanic Technol.*, 26, 1994-2014, doi:10.1175/2009JTECHA1231.1.

Oo, M., and R. Holz (2011), Improving the CALIOP aerosol optical depth using combined MODIS-CALIOP observations and CALIOP integrated attenuated total color ratio, *J. Geophys. Res.*, 116, D14201, doi:10.1029/2010JD014894.

Pan, X., M. Chin, R. Gautam, H. Bian, D. Kim, P. R. Colarco, T. L. Diehl, T. Takemura, L. Pozzoli, K. Tsigaridis, S. Bauer and N. Bellouin (2015), A multi-model evaluation of aerosols over South Asia: common problems and possible causes, *Atmos. Chem. Phys.*, 15, 5903-5928, doi:10.5194/acp-15-5903-2015.

Pappalardo, G. et al. (2010), EARLINET correlative measurements for CALIPSO: first intercomparison results, *J. Geophys. Res.*, 115, D00H19, doi:10.1029/2009JD012147.

Powell, K. A., C. A. Hostetler, Z. Liu, M. A. Vaughan, R. E. Kuehn, W. H. Hunt, K. Lee, C. R. Trepte, R. R. Rogers, S. A. Young, and D. M. Winker (2009), CALIPSO Lidar Calibration Algorithms. Part I: Nighttime 532-nm Parallel Channel and 532-nm Perpendicular Channel, *J. Atmos. Ocean. Tech.*, 26(10), 2015–2033, doi: 10.1175/2009JTECHA1242.1.

Redemann, J., M. A. Vaughan, Q. Zhang, Y. Shinozuka, P. B. Russell, J. M. Livingston, M. Kacenelenbogen, and L. A. Remer (2012), The comparison of MODIS-Aqua (C5) and CALIOP (V2 & V3) aerosol optical depth, *Atmos. Chem. Phys.*, 12, 3025-3043, doi:10.5194/acp-12-3025-2012.

Remer, L., R. G. Kleidman, R. Levy, Y. J. Kaufman, D. Tanré, S. Mattoo, J. V. Martins, C. M. Ichoku, I. Koren, H. Yu, and B. Holben (2008), Global aerosol climatology from the MODIS satellite sensors, *J. Geophys. Res.*, 113, D14S07, doi:10.1029/2007JD009661.

Remer, L. A., Y. J. Kaufman, D. Tanré, S. Mattoo, D. A. Chu, J. V. Martins, R-R. Li, C. Ichoku, R. C. Levy, R. G. Kleidman, T. F. Eck, E. Vermote, B. N. Holben (2005), The MODIS aerosol algorithm, products, and validation, *J. Atmos. Sci.*, 62, 947–973, doi:10.1175/JAS3385.1.

Rogers, R. R., M. A. Vaughan, C. A. Hostetler, S. P. Burton, R. A. Ferrare, S. A. Young, J. W. Hair, M. D. Obland, D. B. Harper, A. L. Cook, and D. M. Winker (2014), Looking Through the Haze: Evaluating the CALIPSO Level 2 Aerosol Optical Depth using Airborne High Spectral Resolution Lidar Data, *Atmos. Meas. Tech.*, 7, 4317-4340, doi:10.5194/amt-7-4317-2014.

Rogers, R. R., C. A. Hostetler, J. W. Hair, R. A. Ferrare, Z. Liu, M. D. Obland, D. B. Harper, A. L. Cook, K. A. Powell, M. A. Vaughan, and D. M. Winker (2011), Assessment of the CALIPSO Lidar 532 nm Attenuated Backscatter Calibration Using the NASA LaRC Airborne High Spectral Resolution Lidar, *Atmos. Chem. Phys.*, 11, 1295-1311, doi:10.5194/acp-11-1295-2011.

Schuster, G. L., M. Vaughan, D. MacDonnell, W. Su, D. Winker, O. Dubovik, T. Lapyonok, and C. Trepte (2012), Comparison of CALIPSO aerosol optical depth retrievals to AERONET measurements, and a climatology for the lidar ratio of dust, *Atmos. Chem. Phys.*, 12, 7431-7452, doi:10.5194/acp-12-7431-2012.

Sekiyama, T. T., T. Y. Tanaka, A. Shimizu, and T. Miyoshi (2010), Data assimilation of CALIPSO aerosol observations, *Atmos. Chem. Phys.*, 10, 39-49, doi:10.5194/acp-10-39-2010.

Sheng, J.-X., D. K. Weisenstein, B.-P. Luo, E. Rozanov, A. Stenke, J. Anet, H. Bingemer, and T. Peter (2015), Global atmospheric sulfur budget under volcanically quiescent conditions: Aerosol-chemistry-climate model predictions and validation, *J. Geophys. Res.*, 120, 256–276, doi:10.1002/2014JD021985.

Smirnov, A., B. N. Holben, T. F. Eck, I. Slutsker, B. Chatenet, and R. T. Pinker (2002), Diurnal variability of aerosol optical depth observed at AERONET (Aerosol Robotic Network) sites, *Geophys. Res. Lett.* , 29 (23), 2115, doi:10.1029/2002GL016305.

Tesche, M., A. Ansmann, D. Müller, D. Althausen, R. Engelmann, M. Hu, and Y. Zhang (2007), Particle backscatter, extinction, and lidar ratio profiling with Raman lidar in south and north China. *App. Opt.*, 46(25), 6302-6308, doi: 10.1364/AO.46.006302.

Thorsen, T. J. and Q. Fu (2015), CALIPSO-inferred aerosol direct radiative effects: Bias estimates using ground-based Raman lidars, *J. Geophys. Res.*, 120, 12,209–12,220, doi:10.1002/2015JD024095.

Toth, T. D., J. Zhang, J. R. Campbell, J. S. Reid, Y. Shi, R. S. Johnson, A. Smirnov, M. A. Vaughan, and D. M. Winker (2013), Investigating enhanced Aqua MODIS aerosol optical depth retrievals over the mid-to-high latitude Southern Oceans through intercomparison with co-located CALIOP, MAN, and AERONET data sets, *J. Geophys. Res.*, 118, 4700–4714, doi:10.1002/jgrd.50311.

Toth, T. D., M. A. Vaughan, J. W. Hair, C. F. Butler, C. A. Hostetler and R. A. Ferrare (2016), Assessing CALIPSO Version 4 Attenuated Backscatter 532 nm Calibration with NASA

LaRC Airborne High Spectral Resolution Lidar Measurements, The AMS 96th Annual Meeting, 10–14 January 2016, New Orleans LA (see https://ams.confex.com/ams/96Annual/webprogram/Paper292226.html)

Uno, I., K. Eguchi, K. Yumimoto, T. Takemura, A. Shimizu, M. Uematsu, Z. Liu, Z. Wang, Y. Hara and N. Sugimoto (2009), Asian dust transported one full circuit around the globe, *Nature Geoscience*, doi:10.1038/NGEO583.

Vaughan, M. A., K. A. Powell, R. E. Kuehn, S. A. Young, D. M. Winker, C. A. Hostetler, W. H. Hunt, Z. Liu, M. J. McGill, and B. J. Getzewich (2009), Fully automated detection of cloud and aerosol layers in the CALIPSO lidar measurements, *J. Atmos. Oceanic Technol.*, 26, 2034–2050, doi:10.1175/2009JTECHA1228.1.

Vernier, J. P., J. P. Pommereau, A. Garnier, J. Pelon, N. Larsen, J. Nielsen, T. Christensen, F. Cairo, L. W. Thomasson, T. Leblanc, and I. S. McDermid (2009), Tropical stratospheric aerosol layer from CALIPSO lidar observations, *J. Geophys. Res.*, 114, D00H10, doi:10.1029/2009JD011946.

Voss, K. J., E. J. Welton, P. K. Quinn, J. Johnson, A. M. Thompson, and H. R. Gordon (2001), Lidar measurements during Aerosols99, *J. Geophys. Res.*, 106(D18), 20821–20831, doi:10.1029/2001JD900217.

Wandinger, U., M. Tesche, P. Seifert, A. Ansmann, D. Müller, and D. Althausen (2010), Size matters: Influence of multiple scattering on CALIPSO light - extinction profiling in desert dust, *Geophys. Res. Lett.*, 37, L10801, doi:10.1029/2010GL042815.

Wang, P.-H., P. Minnis, M. P. McCormick, G. S. Kent, and K. M. Skeens (1996), A 6-year climatology of cloud occurrence frequency from Stratospheric Aerosol and Gas

Experiment II observations (1985–1990), *J. Geophys. Res.*, 101(D23), 29407–29429, doi:10.1029/96JD01780.

Welton, E. J., Voss, K. J., Gordon, H. R., Maring, H., Smirnov, A., Holben, B., Schmid, B., Livingston, J. M., Russell, P. B., Durkee, P. A., Formenti, P. and Andreae, M. O. (2000), Ground-based lidar measurements of aerosols during ACE-2: instrument description, results, and comparisons with other ground-based and airborne measurements, *Tellus B*, 52, 636–651, doi:10.1034/j.1600-0889.2000.00025.x.

Winker, D. M., et al. (2010), The CALIPSO Mission. A Global 3D view of aerosols and clouds, *Bull. Amer. Meteorol. Soc.*, 91(9), 1211–1229,doi:10.1175/2010bams3009.1.

Winker, D. M., J. L. Tackett, B. J. Getzewich, Z. Liu, M. A. Vaughan, and R. R. Rogers (2013), The global 3-D distribution of tropospheric aerosols as characterized by CALIOP, *Atmos. Chem. Phys.*, 13, 3345–3361, doi:10.5194/acp-13-3345-2013.

Young, S. A. (1995), Lidar analysis of lidar backscatter profiles in optically thin clouds. *Appl. Opt.*, 34, 7019–7031, doi: 10.1364/AO.34.007019.

Young, S. A., and M. A. Vaughan (2009), The Retrieval of Profiles of Particulate Extinction from Cloud-Aerosol Lidar Infrared Pathfinder Satellite Observations (CALIPSO) Data: Algorithm Description, *J. Atmos. Oceanic Technol.*, 26(6), 1105–1119, doi:10.1175/2008JTECHA1221.1.

Young, S. A., M. A. Vaughan, R. E. Kuehn, and D. M. Winker (2013), The Retrieval of Profiles of Particulate Extinction from Cloud-Aerosol Lidar Infrared Pathfinder Satellite Observations (CALIPSO) Data: Uncertainty and Error Sensitivity Analyses, *J. Atmos. Oceanic Technol.*, 30, 395-428, doi:10.1175/JTECH-D-12-00046.1.

Yumimoto, K., K. Eguchi, I. Uno, T. Takemura, Z. Liu, A. Shimizu, and N. Sugimoto (2009), Elevated large-scale dust veil originated in the Taklimakan Desert: intercontinental transport and 3-dimensional structure captured by CALIPSO and regional and global models, *Atmos. Chem. Phys.*, 9, 8545-8558, doi:10.5194/acp-9-8545-2009.

Tables

Table 1. Mean (± standard deviation) AODs for MODIS, CALIOP, and retrieved in this study (detected and undetected layers) for constrained retrieval with different altitudes for initiating the retrieval. The numbers of retrieved data with success rates for the retrieval are also shown. The lidar ratios for the constrained retrieval are shown in Figure 3.

	35 km	25 km	15 km	5 km	Layer Top
MODIS	0.135 ± 0.070	0.136 ± 0.070	0.138 ± 0.071	0.137 ± 0.071	0.137 ± 0.072
CALIOP	0.094 ± 0.095	0.094 ± 0.095	0.094 ± 0.094	0.092 ± 0.092	0.092 ± 0.094
Detected layer	0.092 ± 0.074	0.096 ± 0.073	0.103 ± 0.074	0.114 ± 0.071	0.127 ± 0.070
Undetected layer	0.043 ± 0.033	0.040 ± 0.033	0.035 ± 0.032	0.023 ± 0.027	0.010 ± 0.019
No. of data (success rate)	150,467 (0.63)	165,149 (0.69)	180,871 (0.75)	201,819 (0.84)	205,035 (0.85)

Table 2. Mean (± standard deviation) AODs for whole column (retrieved), CALIOP (Level 2 Products), detected and undetected layers (retrieved), and number of data points used for unconstrained retrieval from 35 km AMSL to surface. The estimated lidar ratio for undetected layers of 28.75 sr.

	All	Land	Ocean	Day	Night
Column	0.116±0.149	0.110±0.172	0.121±0.129	0.113±0.150	0.120±0.149
CALIOP	0.070±0.123	0.067±0.152	0.072±0.095	0.067±0.124	0.074±0.122
Detected Layer	0.085±0.139	0.077±0.162	0.091±0.118	0.077±0.131	0.096±0.149
Undetected Layer	0.031±0.052	0.033±0.059	0.030±0.046	0.036±0.066	0.025±0.021
No. of data (success rate)	4,153,384 (0.97)	1,786,665 (0.95)	2,318,241 (0.98)	2,356,336 (0.97)	1,797,048 (0.97)

Figures

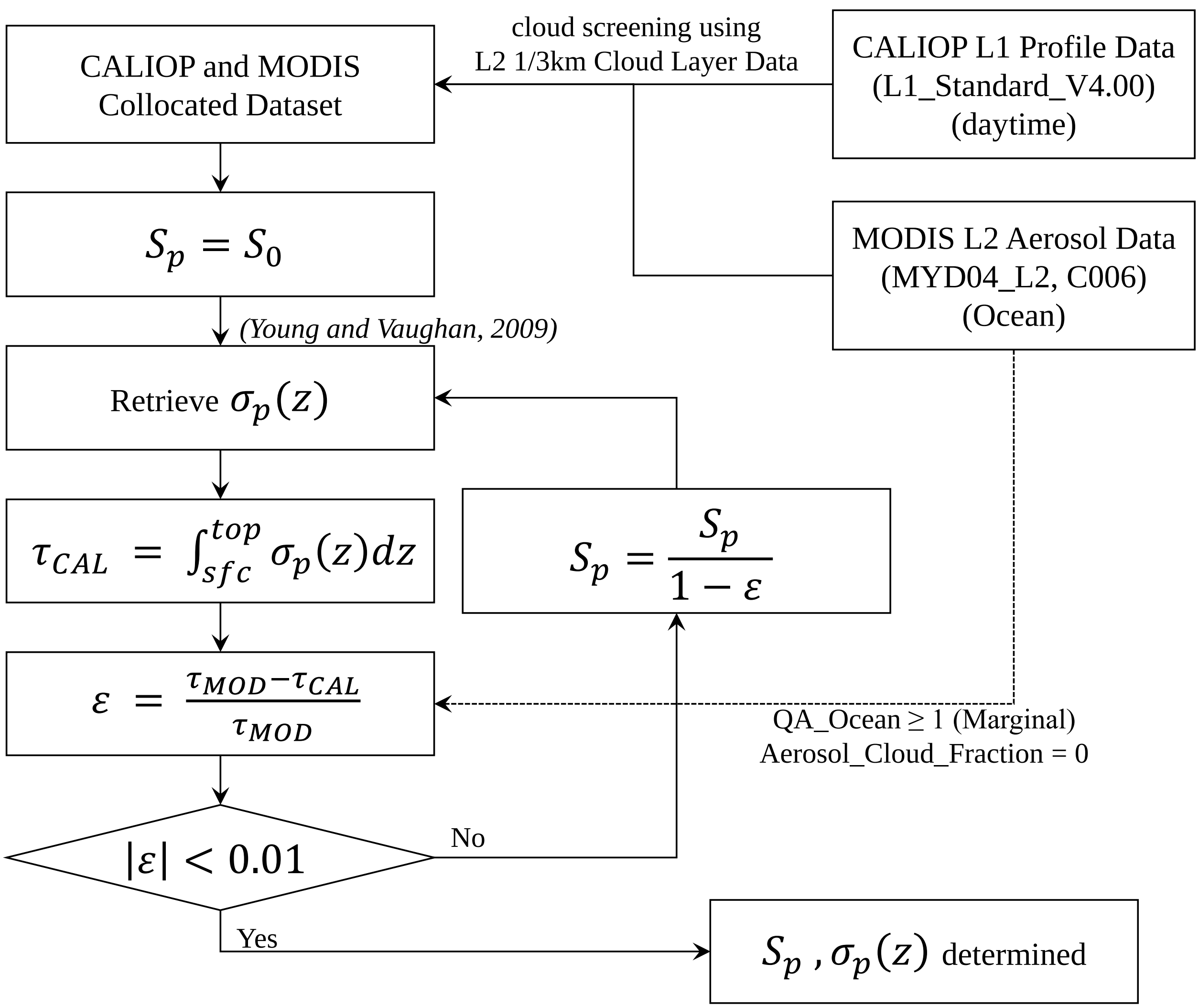

Figure 1. A flowchart for the aerosol extinction retrieval using MODIS AOD as a constraint.

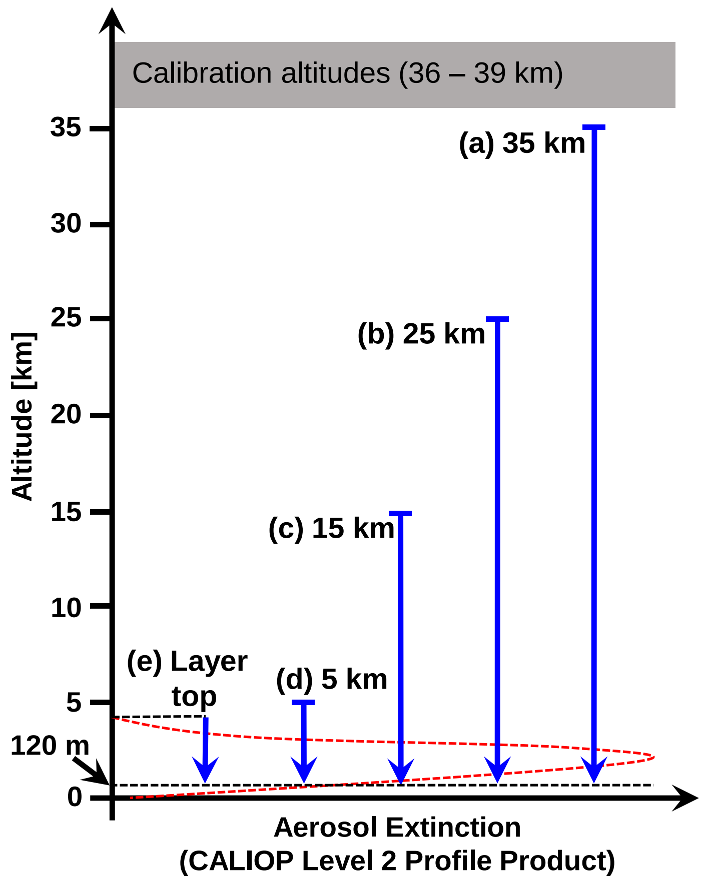

Figure 2. Initial altitudes for the AOD constrained retrieval; from (a) 35 km, (b) 25 km, (c) 15 km, (d) 5 km, and (e) the top of the layer detected by the CALIOP Level 2 algorithm. The lower boundary is 120 m above the surface to avoid contamination by surface returns.

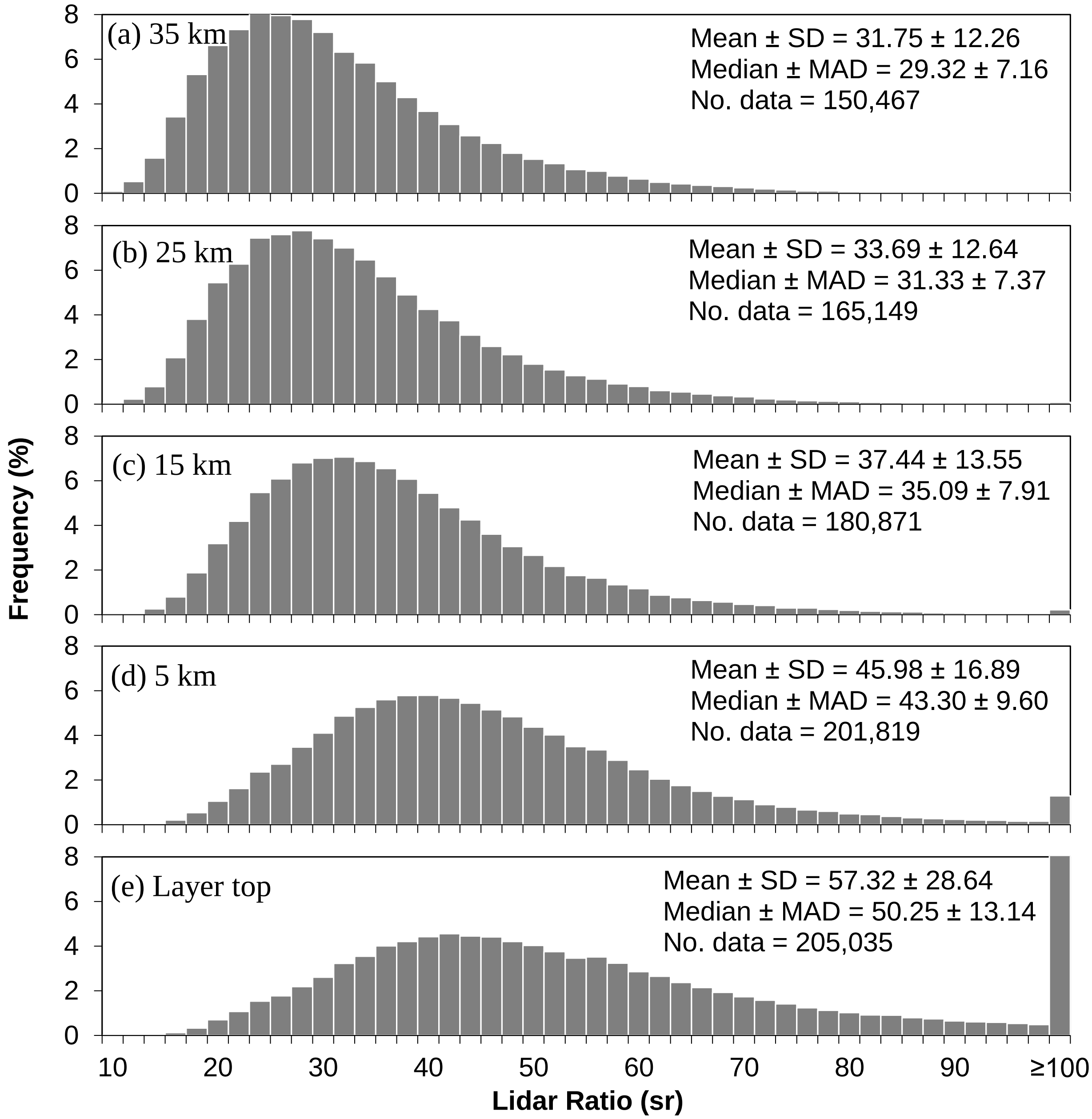

Figure 3. Frequency distributions of aerosol lidar ratio for different initial altitudes shown in Figure 2. Lidar ratios are retrieved from CALIOP Level 1B Product using MODIS AOD as a constraint over ocean from March 2013 to February 2015. The initial altitudes are (a) 35 km, (b) 25 km, (c) 15 km, (d) 5 km, and (e) top of the aerosol layer from the CALIOP Level 2 Product. The mean (± standard deviation), median (± median absolute deviation), and number of data are shown.

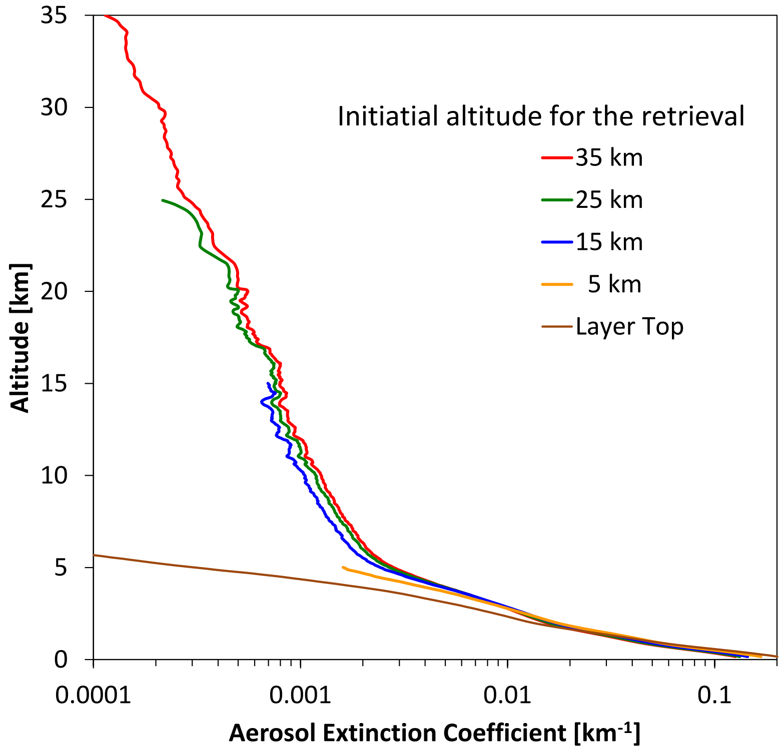

Figure 4. Global mean profiles of total extinction from AOD constrained retrieval for each initial altitude shown in Figure 2 from March 2013 to February 2015.

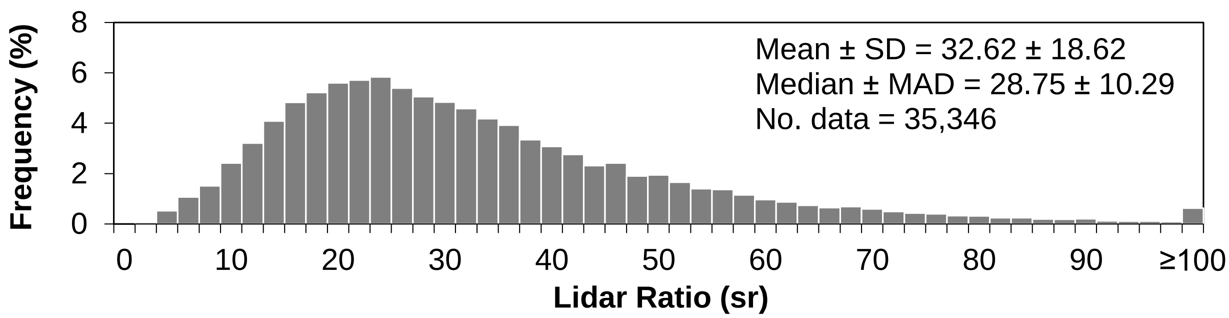

Figure 5. Frequency distributions of aerosol lidar ratio for the undetected layers above marine boundary layer from the AOD constrained retrieval from March 2013 to February 2015. Single layer cases of clean marine aerosol near the surface are selected and the lidar ratio of 23 sr is used for clean marine layer.

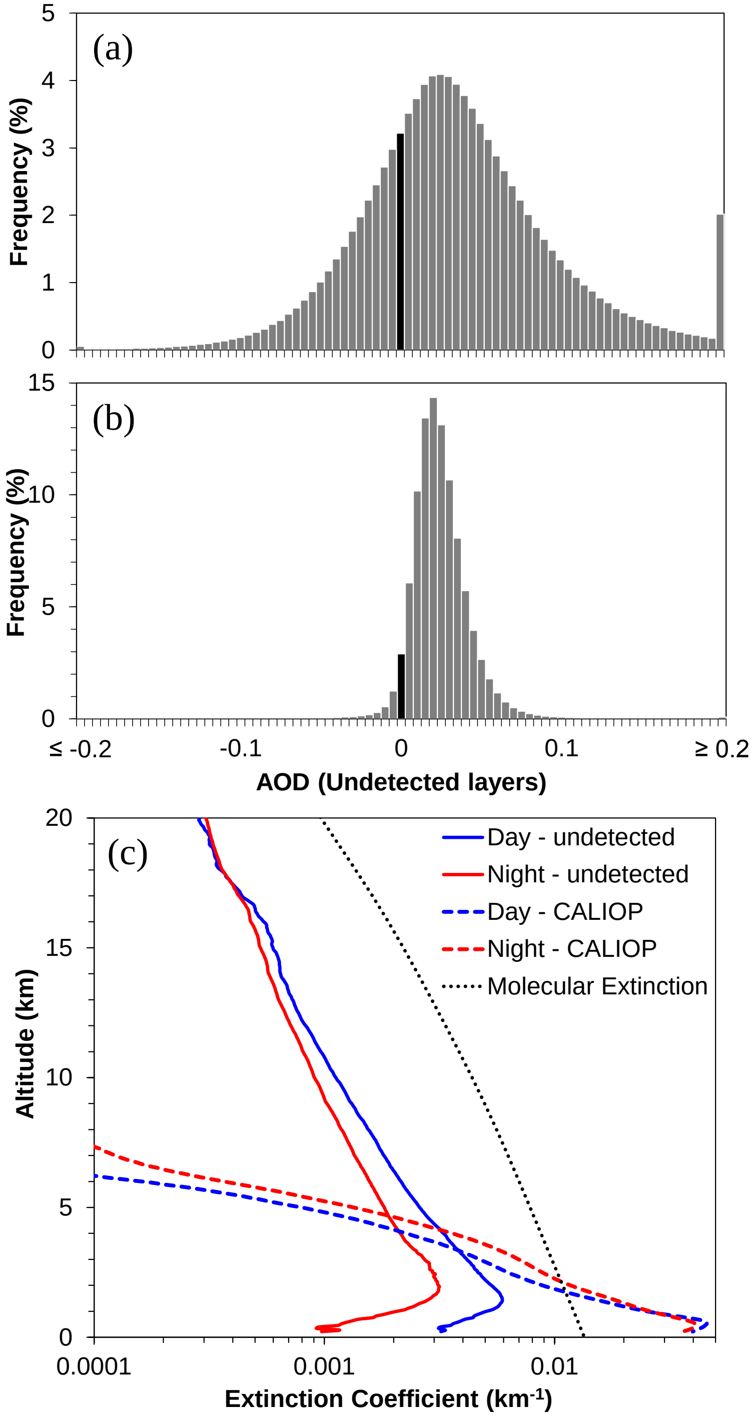

Figure 6. Histograms of global mean ULA for (a) daytime and (b) nighttime retrieved from CALIOP Level 1B Product using an estimated lidar ratio of 28.75 sr from March 2013 to February 2015. The black bar represents a bin at which the undetected layer AOD is zero. (c) Aerosol extinction profiles from CALIOP Level 2 (Version 3.30) Profile Product (dashed lines) and undetected layers retrieved in this study (solid lines). Blue and red represent daytime and nighttime, respectively. Global mean molecular extinction (Rayleigh scattering) is shown in black dotted line.

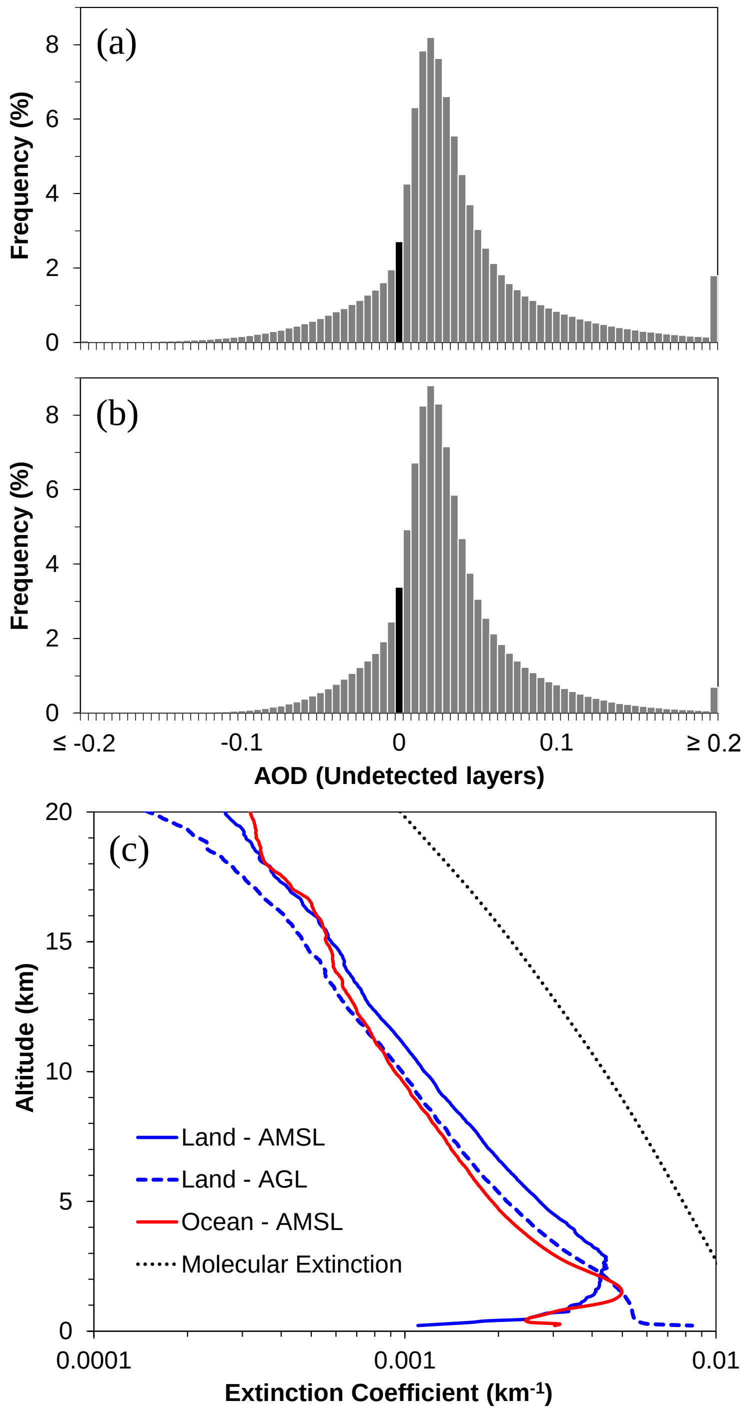

Figure 7. Same as Figure 6 but over (a) land and (b) ocean. (c) Aerosol extinction profiles for the undetected layers over land (blue-solid) and ocean (red-solid) above mean sea level (AMSL). Blue-dashed line is for land above ground level (AGL).

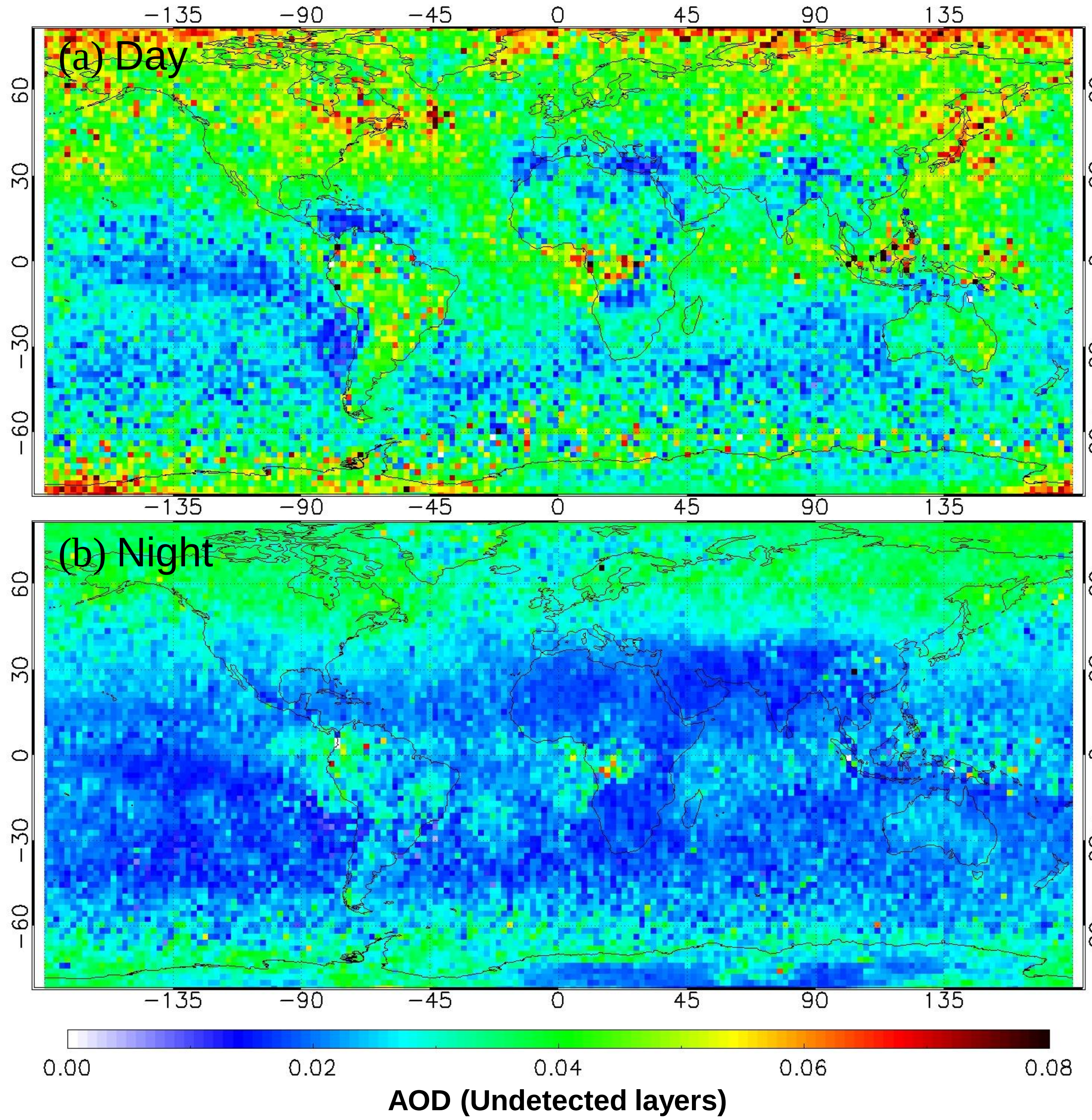

Figure 8. Global distributions of ULA for (a) daytime and (b) nighttime retrieved using estimated lidar ratio of 28.75 sr from March 2013 to February 2015.

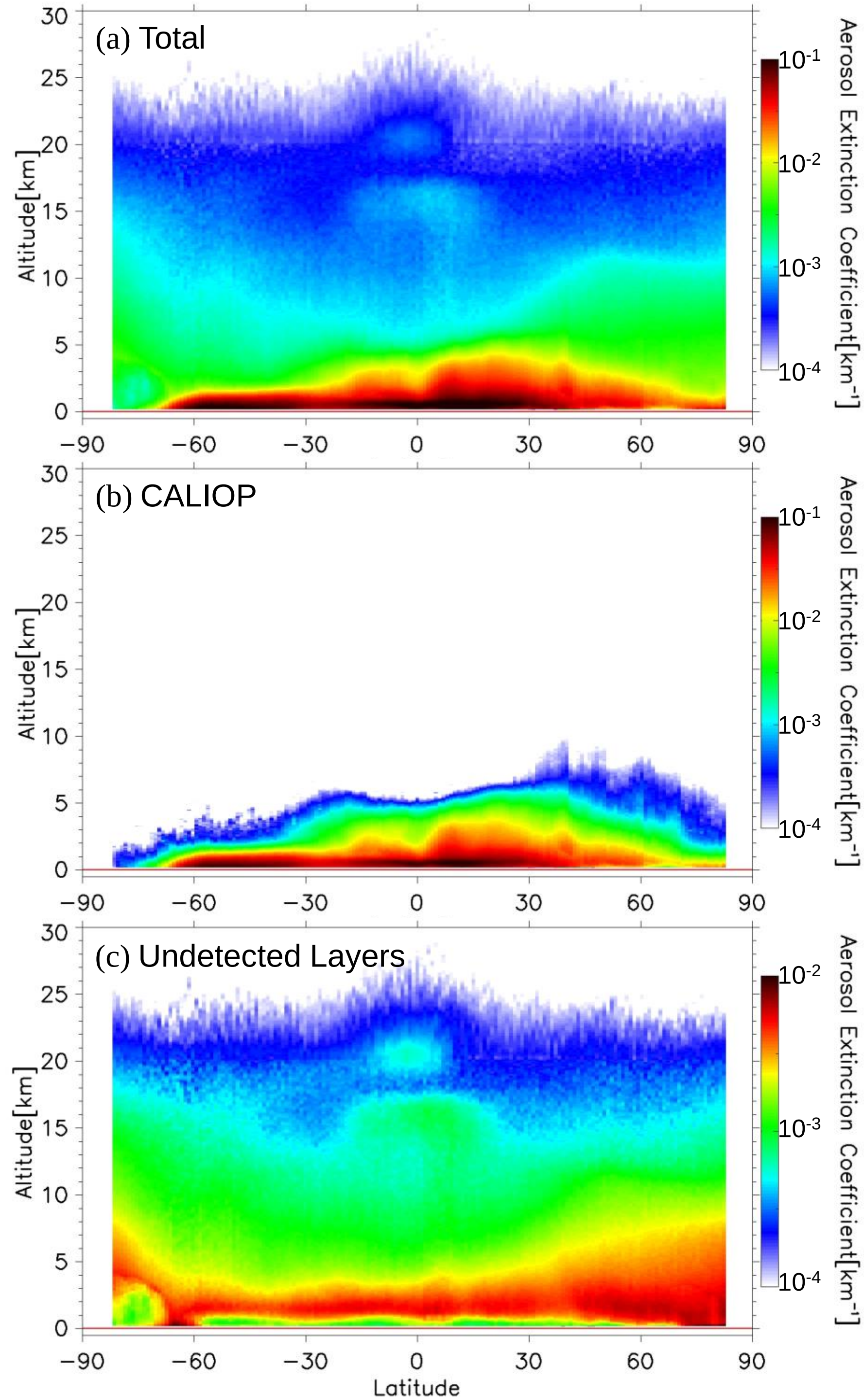

Figure 9. Distribution of zonal mean aerosol extinctions for (a) total, (b) detected, and (c) undetected layers from March 2013 to February 2015. (a) and (c) are retrieved in this study but (b) is from the CALIOP Level 2 Profile Products. Altitudes are AMSL and the highest color scale for (c) is 10 times smaller than (a) and (b).

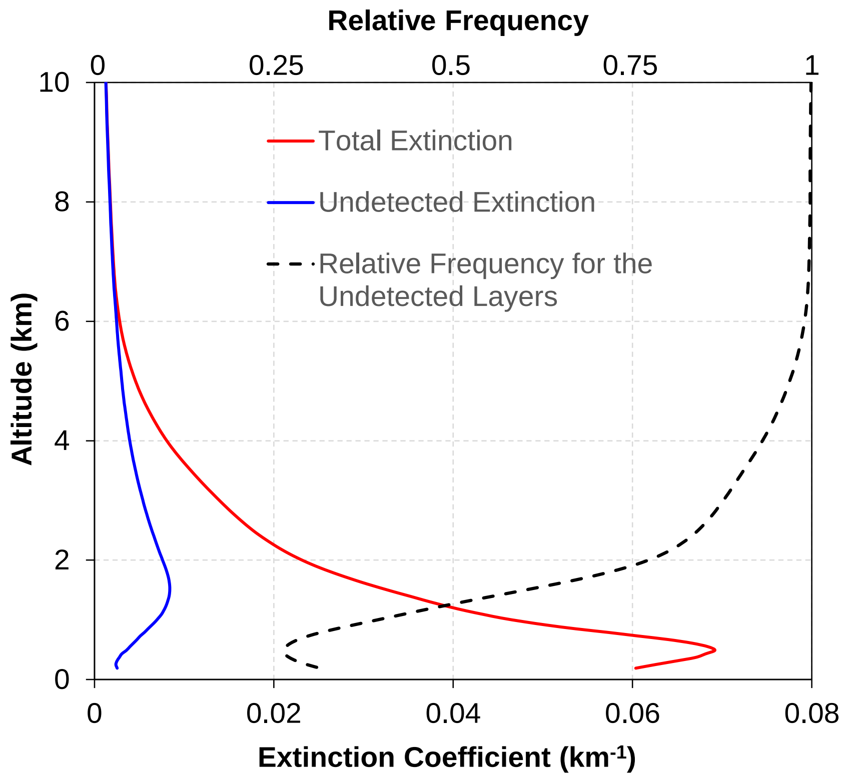

Figure 10. Aerosol extinction profiles for total (red) and undetected layers (blue). Black dashed line is relative frequency of the undetected layers.

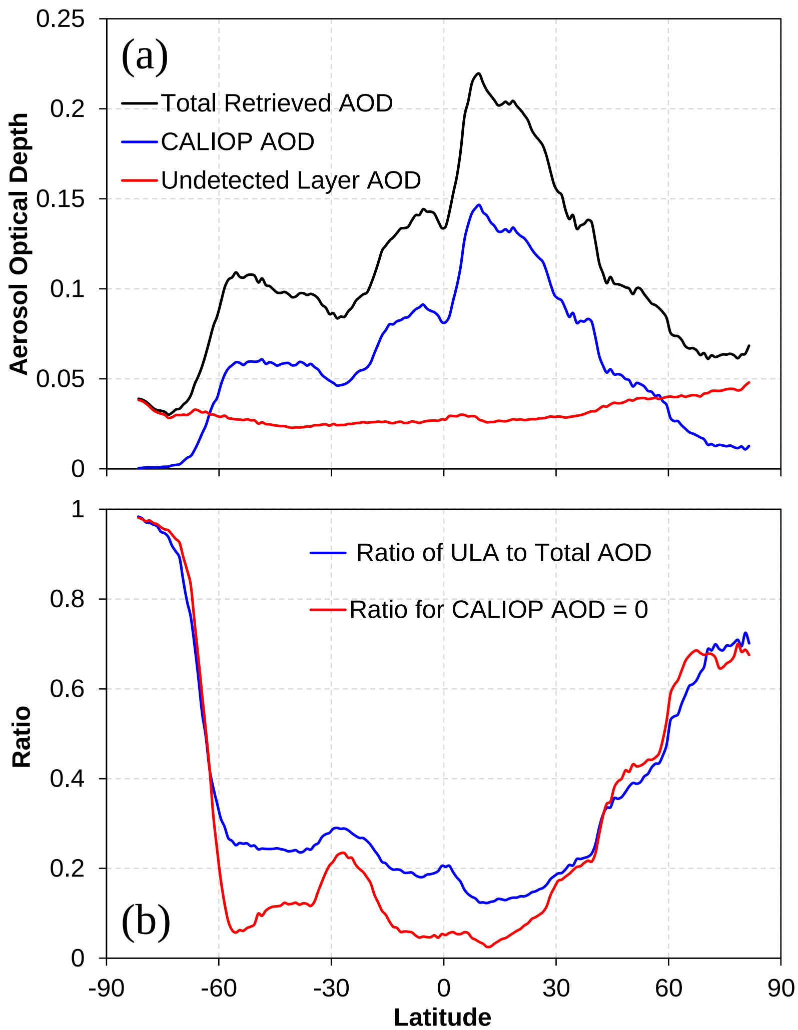

Figure 11. (a) Zonal mean total (detected + undetected) AOD (black), CALIOP AOD (blue), and ULA (red). (b) Relative frequency of cases that CALIOP does not detect any aerosol layers (AOD = 0) for horizontal averaging of 20 km (red) and ratio of undetected layer AOD to total AOD (blue).

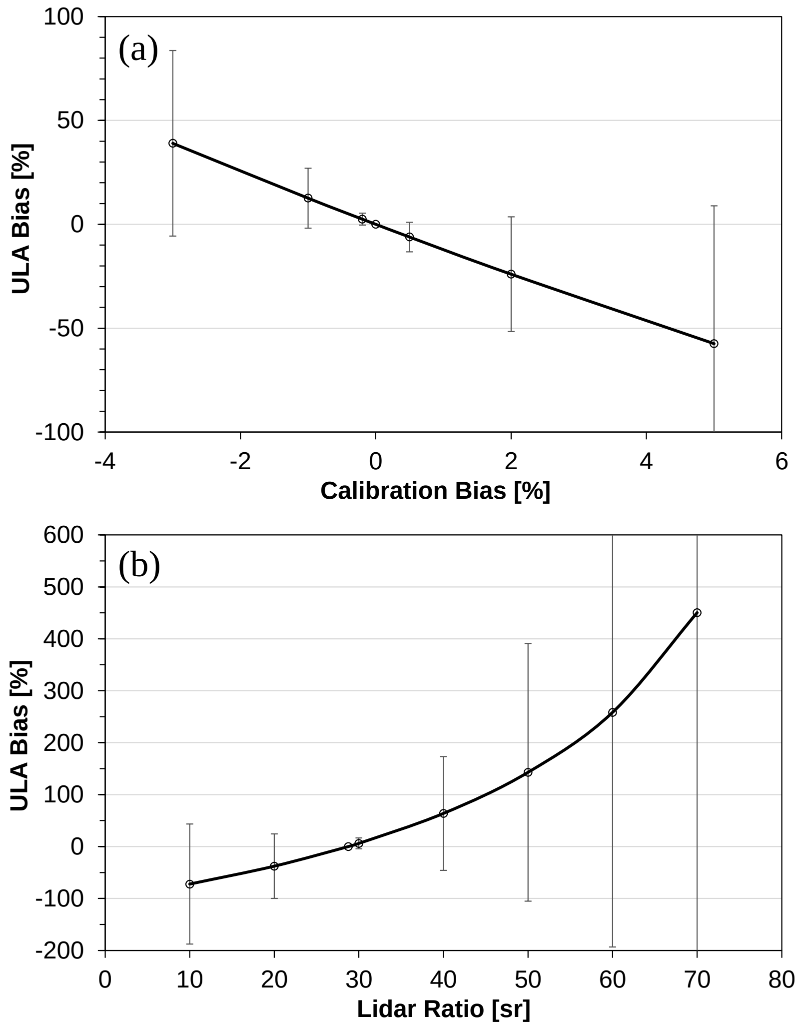

Figure 12. Relative bias in ULA depending on (a) calibration bias and (b) lidar ratio expressed the difference in ULA from the value estimated using a lidar ratio of 28.75 sr. Error bars are standard deviations.